









**ESC**European Society
of CardiologyCardiovascular Research (2020) **116**, 1288–1299

doi:10.1093/cvr/cvz239

High-density lipoprotein remodelled in hypercholesterolaemic blood induce epigenetically driven down-regulation of endothelial HIF-1 α expression in a preclinical animal model

Soumaya Ben-Aicha ^{1,2}, Rafael Escate ^{1,3}, Laura Casaní ¹, Teresa Padró ^{1,3}, Esther Peña ^{1,3}, Gemma Arderiu ¹, Guiomar Mendieta ^{1,2,4}, Lina Badimón^{1,3,5†}, and Gemma Vilahur ^{1,3*†}

¹Cardiovascular Program—ICCC, Research Institute-Hospital de la Santa Creu i Sant Pau, IIB-Sant Pau, Barcelona, Spain; ²School of Medicine, University of Barcelona (UB), Barcelona, Spain; ³Centro de Investigación Biomédica en Red Cardiovascular (CIBERCV), Instituto de Salud Carlos III, Madrid, Spain; ⁴Cardiology Department, Hospital Clinic Barcelona, Barcelona, Spain; and ⁵Cardiovascular Research Chair, Universidad Autónoma Barcelona (UAB), Barcelona, Spain

Received 3 May 2019; revised 24 July 2019; editorial decision 23 August 2019; accepted 29 August 2019; online publish-ahead-of-print 30 August 2019

Time for primary review: 31 days

Aims

High-density lipoproteins (HDLs) are circulating micelles that transport proteins, lipids, and miRNAs. HDL-transported miRNAs (HDL-miRNAs) have lately received attention but their effects on vascular cells are not fully understood. Additionally, whether cardiovascular risk factors affect HDL-miRNAs levels and miRNA transfer to recipient cells remains equally poorly known. Here, we have investigated the changes induced by hypercholesterolaemia on HDL-miRNA levels and its effect on recipient endothelial cells (ECs).

Methods and results

Pigs were kept on a high-fat diet (HC; $n = 10$) or a normocholesterolaemic chow (NC; $n = 10$) for 10 days reaching cholesterol levels of 321.0 (229.7–378.5) mg/dL and 74.0 (62.5–80.2) mg/dL, respectively. HDL particles were isolated, purified, and quantified. HDL-miRNA profiling ($n = 149$ miRNAs) of HC- and NC-HDLs was performed by multipanel qPCR. Cell cultures of porcine aortic ECs were used to determine whether HDL-miRNAs were delivered to ECs. Potential target genes modulated by miRNAs were identified by bioinformatics and candidate miRNAs were validated by molecular analysis. *In vivo* effects in the coronary arteries of normocholesterolaemic swine administered HC- or NC-HDLs were analysed. Among the HDL-miRNAs, four were found in different amounts in HC- and NC-HDL ($P < 0.05$). miR-126-5p and -3p and miR-30b-5p (2.7 \times , 1.7 \times , and 1.3 \times , respectively) were found in higher levels and miR-103a-3p and miR-let-7g-5p (-1.6 \times , -1.4 \times , respectively) in lower levels in HC-HDL. miR-126-5p and -3p were transferred from HC-HDL to EC (2.5 \times ; $P < 0.05$), but not from NC-HDL, by a SRB1-mediated mechanism. Bioinformatics revealed that HIF1 α was the miR-126 target gene with the highest predictive value, which was accordingly found to be markedly reduced in HC-HDL-treated ECs and in miR126 mimic transfected ECs. *In vivo* validation confirmed that HIF1 α was diminished in the coronary endothelial layer of NC pigs administered HC-HDL vs. those administered NC-HDL ($P < 0.05$).

Conclusion

Hypercholesterolaemia induces changes in the miRNA content of HDL enhancing miR126 and its delivery to ECs with the consequent down-regulation of its target gene HIF1 α .

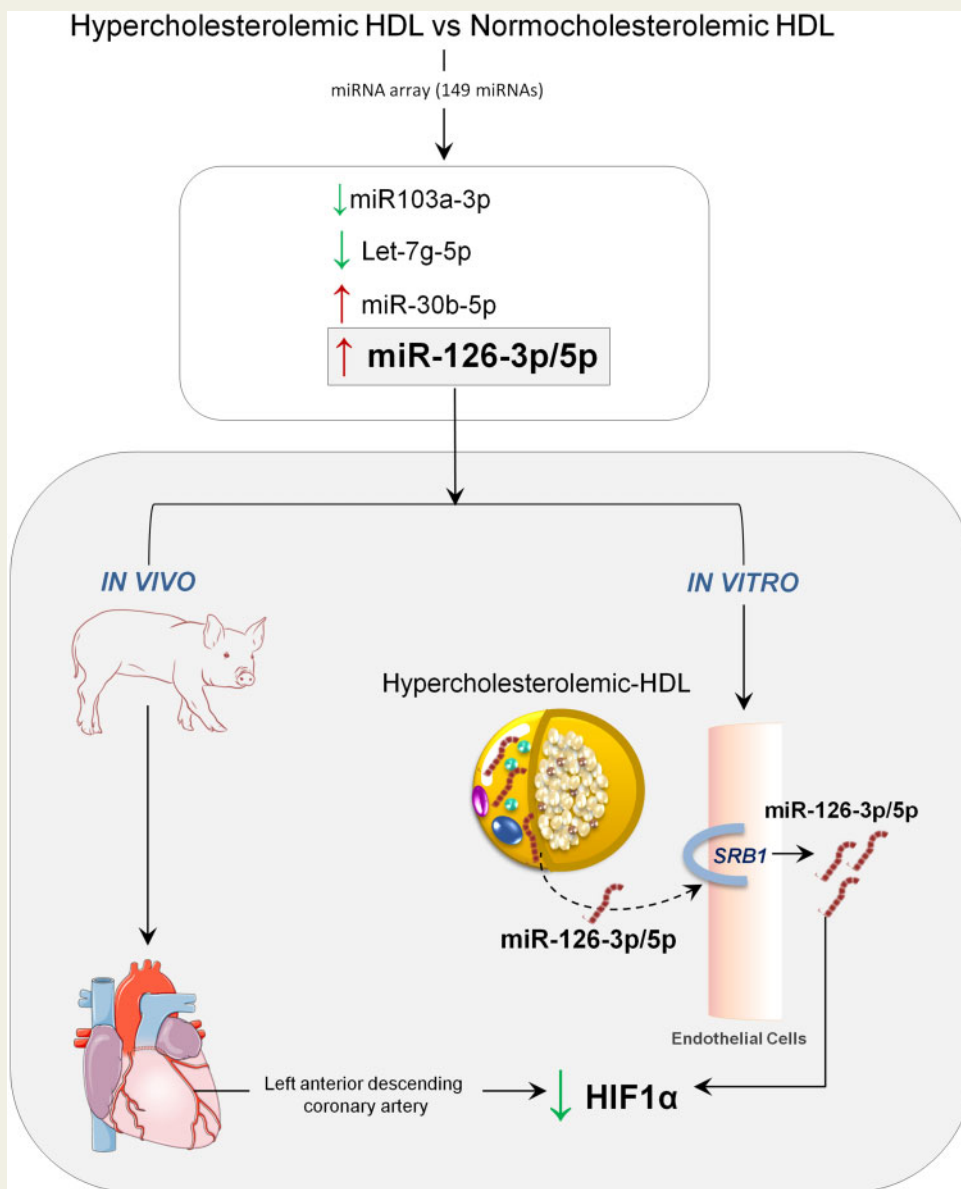
* Corresponding author. Tel: +34 93 5537100; fax: +34 935565559, E-mail: gvilahur@santpau.cat

† The last two authors contributed equally to the work.

© The Author(s) 2019. Published by Oxford University Press on behalf of the European Society of Cardiology.

This is an Open Access article distributed under the terms of the Creative Commons Attribution Non-Commercial License (<http://creativecommons.org/licenses/by-nc/4.0/>), which permits non-commercial re-use, distribution, and reproduction in any medium, provided the original work is properly cited. For commercial re-use, please contact journals.permissions@oup.com

Graphical Abstract



Keywords

HDL • Dyslipidaemia • Translational research • miRNAs • Endothelial cells

1. Introduction

MicroRNAs (miRNAs) are short, non-coding RNAs (~22 nucleotide in length) that control gene expression through post-transcriptional regulation of target mRNAs. Extracellular miRNAs have been detected in multiple lipid-based carriers including exosomes, microparticles, and lipoproteins.¹ Indeed, high-density lipoproteins (HDLs) are lipoproteins that in addition to cholesterol, transport other lipid species, proteins, and miRNAs.² HDL particles exert multiple cardiovascular protective functions. Under physiological conditions HDL-cargo molecules that maintain cardiovascular homeostasis and function by promoting circulating cells, endothelial cells (ECs), vessel wall stabilization, and regulating

reverse cholesterol transport and ischaemia/reperfusion injury.³⁻⁵ In this regard, HDL-mediated transport and delivery of miRNAs to recipient cells can regulate expression of genes involved in lipid metabolism, inflammation, angiogenesis, and apoptosis.⁶⁻⁹

Robust epidemiological data supports that increasing HDL-cholesterol (HDL-c) levels predict improved cardiovascular outcomes; however, HDL-c raising therapies in secondary prevention trials have failed to demonstrate cardiovascular benefits.¹⁰ As such, within the last decade, it has become increasingly evident that the measure of the cholesterol levels transported by HDL (HDL-c) is not a good read-out of HDL beneficial effects because the presence of excess cholesterol (hypercholesterolaemia) increases the transport of cholesterol in detriment of

other beneficial cargos. Moreover, the presence of comorbidities modifies HDL particle composition and function hampering HDL-beneficial effects and even becoming deleterious.^{11–16} We have recently demonstrated that HDL *in vivo* remodelling is affected by low-density lipoprotein (LDL) cholesterol levels. Indeed, the presence of hypercholesterolaemia influences HDL lipidomic and proteomic profile and renders HDL particles dysfunctional.^{17–19} Particularly, HDL particles formed under hypercholesterolaemic conditions, as compared to HDL particles formed in a normocholesterolaemic milieu, have lower levels of phosphatidylcholine-lipid species and higher levels of cholesteryl esters and a lower cargo of several proteins with known cardioprotective functions including lipocalin retinol binding protein-4 and apolipoprotein-M. Interestingly, we have further proved that such adverse structural remodelling is associated with a marked reduction in HDL anti-oxidant and cholesterol efflux capacity and complete loss of HDL-induced cardioprotection.²⁰ However, to date, there is no information on the impact of hypercholesterolaemia on HDL-transported miRNA (HDL-miRNA) content or on the possible effects of HDL-miRNAs on EC gene regulation. Accordingly, in the present study, we aimed to investigate the HDL-miRNA cargo of HDL formed *in vivo* in hypercholesterolaemic conditions and whether the tentative modifications were able to differentially regulate gene expression in target cells.

2. Methods

Experimental procedures were reviewed and approved by the Institutional Animal Care and Use Committees (CEEA-IR) and authorized by the Animal Experimental Committee of the local government (#5601) in accordance to the Spanish law (RD 53/2013) and European Directive 2010/63/EU. In addition, the investigation conforms to the Guide for the Care and Use of Laboratory Animals published by the US National Institutes of Health (NIH Publication No. 85-23, revised 1985), follows the ARRIVE guidelines and is committed to the 3Rs of laboratory animal research and consequently used the minimal number of animals to reach statistical significance.²¹ All animals were allowed to acclimate 7 days prior to any intervention and housed in individual cages under light-controlled conditions and room temperature.

2.1 Experimental model of hypercholesterolaemia and HDL isolation

2.1.1 Experimental animal model

Four-month-old pigs ($N = 20$; weight: ≈ 40 kg) randomly received either regular normocholesterolaemic chow (NC; $n = 10$) or a high-fat/high-cholesterol diet (HC; $n = 10$) for 10 days (composition of the diet is detailed in [Supplementary material online, Table S1](#)). HC animals developed high LDL-cholesterol levels similar to those found in hypercholesterolaemic humans, 321.0 (229.7–378.5) mg/dL, while NC-animals had 74.0 (62.5–80.2) mg/dL ($P < 0.0001$; [Supplementary material online, Table S2](#)).²²

2.1.2 HDL isolation and purification

On Day 10, animals were tranquilized by intramuscular injection of Azoperone (40 mg/mL; 7 mg/kg), anaesthesia was induced by propofol (2%; 3 mg/kg), and maintained by isoflurane inhalation (3%). Animals were then sacrificed by propofol overdose and potassium chloride (2M). HDLs were isolated by standard sequential preparative ultracentrifugation techniques from plasma-EDTA (ethylenediaminetetra-acetic acid) before sacrifice as previously reported.¹⁹ Protein levels in HDL were quantified by standard Bradford protein assay (PierceTM BCA

Protein Assay Kit, Thermo Fisher Scientific, Waltham, Massachusetts, USA). Lipoprotein cholesterol content was assessed by the Cholesterol Quantification Kit (MAK043-Sigma-Aldrich; MO, USA). The purity of the HDL fraction was confirmed by excluding the presence of ApoB (by-agarose gel electrophoresis), microvesicles (FACS for Anexin V+ microvesicles), and exosomes (western blots for transpanins CD63 and CD81; exosomes isolated by ExoMirTM Kit).²³

2.1.3 HDL miRNA isolation

HDL samples were thawed on ice and centrifuged at 3000 g for 5 min at 4°C. An aliquot of 200 μ L per sample (protein concentration HC: 5.7 μ g/ μ L and NC: 5.6 μ g/ μ L) was transferred to a FluidX tube and 60 μ L of lysis solution buffer containing 1 μ g carrier-RNA per 60 μ L lysis solution buffer and RNA spike-in template mixture were added to the sample and mixed for 1 min and incubated for 7 min at room temperature, followed by addition of 20 μ L protein precipitation solution buffer. Total RNA was extracted from the samples using miRCURY RNA isolation Kit through a high throughput bead-based protocol v.1 (Exiqon, Vedbaek, Denmark) in an automated 96-well format. The purified total RNA was eluted in a final volume of 50 μ L and its optimal quality checked.

2.1.4 HDL miRNA analysis by qPCR

Seven microlitres of RNA were reverse transcribed in 35 μ L reactions using the miRCURY LNATM Universal RT microRNA PCR, Polyadenylation and cDNA synthesis kit (Exiqon). cDNA was diluted 50 \times and assayed in 10 μ L PCR reactions according to the protocol for miRCURY LNATM Universal RT microRNA PCR. A panel of 149 miRNAs homologous for pig and human were analysed in HDL ([Supplementary material online, Table S3](#)). Each miRNA was assayed by qPCR (microRNA Ready-to-Use PCR, Custom Pick and Mix panel using ExiLent SYBR[®] Green master mix) and negative controls were run in parallel. The amplification was performed in a LightCycler[®] 480 Real-Time PCR System (Roche) in 384-well plates. The amplification curves were analysed using the Roche LC software, both for Cq determination (following the 2nd derivative method) and for melting curve analysis.

2.1.5 HDL miRNA data analyses

The amplification efficiency was calculated (LinReg software). All assays were inspected for distinct melting curves and the Melt temperature (T_m) was checked to be within known specifications for the assay. Assays had to be detected beyond 5 Cqs of the negative control and with $Cq < 37$ in order to be included in the data analyses. The NormFinder helped to find out the best possible normalizer which resulted to be the average of the best assays detected in all samples ($n = 20$). The formula used to calculate the normalized Cq values was the following: Normalized Cq = average Cq ($n = 20$) - assay Cq (sample). We then performed a comparative analysis between NC and HC isolated HDL-miRNAs. Data were expressed as fold-change.

2.2 Cell culture studies

2.2.1 Porcine aortic endothelial cells isolation, expansion and treatment

Aortic ECs were obtained from regular-fed pigs by collagenase digestion as previously described.²⁴ Cells were cultured in growth M199 (Gibco) medium supplemented with 10% FBS and antibiotics (0.1 mg/mL streptomycin, 100 U/mL penicillin) until confluence. Cells were detached by trypsin/EDTA treatment and seeded into larger flasks for expansion.

Forty-eight hours after plating 300 000 cells in six well plates, 0.1% FBS was added to the medium for 24 h and then EC were incubated with NC-HDL (50 μ g/mL protein), HC-HDL (50 μ g/mL protein), or PBS/control for 18 h (in duplicates; $n = 5$) as previously reported.^{24,25} EC viability was determined by trypan blue exclusion. ECs were always used between the third and seventh passage.

2.2.2 ECs and plasma miRNA isolation and data analysis

ECs were collected and total RNA was obtained with mirVANA miRNA kit. The RNA was transcribed using TaqMan[®] Advanced miRNA cDNA Synthesis Kit (Applied Biosystems; CA, EU) protocol. All assays were performed in duplicates for the differentially expressed miRNAs including miR-126-5p and -3p, let7g-5p, miR-103a-3p and miR-30b-5p (Life Technologies; CA, EU) ($n = 5$). For normalization miR-423-3p and let-7a-5p means were used as endogenous miRNA controls.²⁶ The amplification was performed in ABI PRISM 7900HT Sequence Detection System (Applied Biosystems; CA, EU) in 384-well plates. The amplification curves were analysed using the Applied Biosystems Sequence Detection System 2.4.1 software. Ct values were obtained and processed by the standard curve method and normalized with the endogen. To obtain fold difference vs. control the ratio sample/control was calculated. Networks, functional analyses, detection of miRNAs targets and interactions were generated by Ingenuity Pathway Analysis software (IPA) and RNA hybrid tool.

2.2.3 Assessment of HDL-miRNA transfer to ECs

To investigate whether the scavenger receptor class B member 1 (SRB1) was involved in HDL-miRNA transfer to ECs a specific SRB1 blocker, BLT1 (EMD Millipore Corp, USA; 8 μ M), was added to ECs prior to HDL incubation.²⁵ In addition, and taking into consideration that miR-126 (both 5p and 3p) is encoded in the 7th intron of the EGFL7 gene, we assessed the expression of both EGFL7 and the pre-miRNA sequence (pre-miR-126; $n = 5$) in ECs in order to ascertain whether the potential intracellular changes detected in miR-126-5p and -3p expression were related to an up-regulation of its cellular synthesis or because of transfer from HDL. Pri-miR126 could not be investigated because there is no commercial assay available for *Sus scrofa* so far.

2.3 miR126 target gene analysis

2.3.1 In silico analysis

Potential target genes were obtained by using databases TargetScan, miRwalk (5UTR, CDS, 3UTR) and the Ingenuity Pathway Analysis (IPA; <http://www.ingenuity.com/>), according to their search algorithms. The functionality of target genes in cellular processes was predicted by IPA Core analysis. Furthermore, RNAhybrid (Bielefeld University Bioinformatics server) was used for calculating minimum free energy (MFE), which indicates the accessibility of miRNAs at the target gene binding sites. Target genes were selected by comparison of MFE values.²⁷

2.3.2 Gene expression validation

RNA was transcribed using the High Capacity cDNA Archive kit (Applied Biosystems, Foster City, CA, USA) protocol for genomic RNA. qPCRs were performed in duplicates for SCARB1, miR-126-5p and -3p, HIF1 α , vascular cell adhesion protein 1 (VCAM1), vascular endothelial growth factor A (VEGFA) (Life Technologies; CA, EU), and EGFL7 (Bio-Rad Laboratories, CA, EU). 18S rRNA was used as endogenous control for tissue samples and GAPDH (Life Technologies; CA, EU) for EC

samples. The amplification was performed in ABI PRISM 7900HT Sequence Detection System (Applied Biosystems; CA, EU) in 384-well plates. The amplification curves were analysed using the Applied Biosystems Sequence Detection System 2.4.1 software. Ct values were obtained and processed by the standard curve method and normalized with the endogenous gene.

2.3.3 Protein expression validation

Cell lysis was performed according to the previous established protocol.²⁸ The cell protein lysates were stored at -80°C until use. Protein concentrations were assessed using the BSA assay and then SDS-polyacrylamide gel electrophoresis (SDS-PAGE) was run. Blots were blocked with BSA at room temperature for 1 h and incubated with the appropriate primary antibody [HIF1 α (sc-10790, Santa Cruz Biotechnology, Dallas, TX, USA)] at 4°C overnight. Membranes were then incubated with a horseradish peroxidase-conjugated anti-mouse antibody for 2 h. Densitometry analyses were performed using commercially available quantitative software (ImageLab Software, Bio-Rad Laboratories, CA, USA) with the control representing 1.0-fold.

2.3.4 Mir126 target validation by miR126-mimic and miR126 inhibitor

ECs were transfected with miR126-mimic or miR126 inhibitor (both for -5p and -3p) (Life Technologies; CA, EU) with the Lipofectamine[™] RNAiMAX Transfection Reagent (Life Technologies; CA, EU) following the supplier recommendations. Then, ECs were treated with HDL-HC or HDL-NC as reported above. A miRNA Mimic Negative Control #1 (Life Technologies; CA, EU) was run in parallel.

2.4 In vivo validation of miR-126 target genes by confocal microscopy

We assessed HIF1 α protein expression in the coronary arteries of normocholesterolaemic pigs ($n = 12$) administered HC-HDL ($n = 6$) or NC-HDL ($n = 6$). In this regard, we processed the coronary arteries from pigs of our previous published study¹⁹ which had been kept in our tissue biobank at -80°C until use. Accordingly, we fixed the proximal portion of the coronary artery of all pigs in 4% paraformaldehyde and the paraffin-embedded for confocal microscopy analysis. Serial sections (5 μ m thick) were incubated with blocking buffer and then with antibody against HIF1 α (H1alpha67, Novus Biologicals, Littleton, CO, USA). Preparations were counterstained with fluorescently labelled secondary antibody (Invitrogen) and mounted with fluorescent medium. Fluorescent images were acquired in a scan format of 1024 \times 1024 pixels in a spatial data set ($x y z$). Controls with no primary antibody showed no fluorescence labelling.

2.5 Statistics

The Shapiro–Wilk test was employed to analyse data normal or non-normal distribution; data are reported as the mean \pm standard deviation and median (interquartile range), respectively. For the biochemical descriptive data and SRB1 *in vivo* analysis, we performed non-parametric test Kruskal–Wallis with Dunn's multiple comparisons corrected test. Tukey's honest significance corrected test was used in conjunction with an ANOVA (*post hoc* analysis) for multiple comparisons to find significantly difference between group means due to its condition of independent samples. Accordingly, *t*-test was used for two group independent samples mean comparison. A two-sided *P*-value less than 0.05 was considered statistically significant.

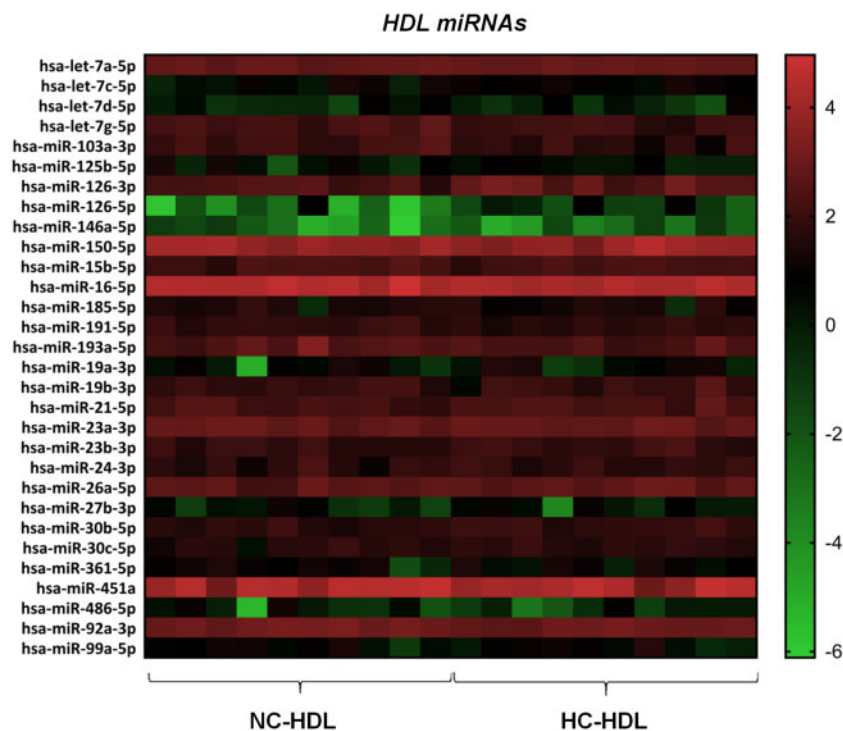


Figure 1 HeatMap including the miRNAs detected in all HDL samples isolated from hypercholesterolaemic (HC; $n = 10$) and normocholesterolaemic (NC; $n = 10$) pigs.

Sample size: For the EC approach accepting α risk of 0.05 and β risk of 0.2 in a two-sided test, an $n = 3$ was necessary to recognize as statistically significant difference ≥ 0.5 units. Yet, we performed $n = 5$ in all conditions to make our conclusions more robust. The common standard deviation is assumed to be 0.2 and it we anticipated a dropout rate of 0% (GRANMO software, Spain). All statistical analyses and graphics were performed using GraphPad Prism 7.0 version software.

3. Results

3.1 HDL-characterization

Cholesterol content was two-fold higher in HC- than in NC-HDLs (Supplementary material online, Table S4). This observation is in line with our previous findings regarding the effects of hypercholesterolaemia on modifying HDL-lipid composition.²⁰ The isolated HDL samples were free from ApoB (Supplementary material online, Figure S1A), Annexin V+ microvesicles (Supplementary material online, Figure S1B), and exosomes (Supplementary material online, Figure S1C), supporting the purity of the HDL preparations. The protein concentration was similar in HC-HDL (5.7 $\mu\text{g}/\mu\text{L}$) and in NC-HDL (5.6 $\mu\text{g}/\mu\text{L}$).

3.2 HDL-related miRNA profile

Among the 149 miRNAs analysed, 30 miRNAs were detected in all HDL samples (Figure 1 and Supplementary material online, Table S5). Among these 30 miRNA, the amounts of five miRNAs were significantly different in HC- and in NC-HDL particles ($P < 0.05$). Particularly, there was a higher content of miR126-5p, miR126-3p, and miR-30b-5p in HC-HDL particles as compared to NC-HDL (2.7 \times , 1.7 \times , and 1.3 \times , respectively),

whereas, conversely, the amounts of miR103a-3p and let7g-5p were significantly lower (-1.6 \times , -1.4 \times , respectively).

3.3 HC-HDL particles transfer miR-126 to ECs through a SRB1-dependent mechanism

ECs incubated with HC-HDL showed significantly higher intracellular levels of miR-126-5p ($P < 0.0001$) and miR126-3p ($P < 0.0001$), while levels of both miR-126s (5p and 3p) were similar in control ECs and ECs incubated with NC-HDL (Figure 2A and B). No differences were observed for miR103a-3p (Figure 2C), miR30b-5p (Figure 2D), and let7g-5p (Figure 2E).

Interestingly, the internalization of miRNA-126 in ECs was mediated by SRB1. We found that SRB1 blockade by BLT-1 abolished HC-HDL-induced increase in miR-126 (both 5p and 3p) (Figure 3A and B) content. SRB1 expression in ECs did not differ by incubation with either NC- or HC-HDLs (Supplementary material online, Figure S2A). Moreover, comparable SRB1 transcript levels were detected in pig coronary arteries and liver (Supplementary material online, Figure S2B). Therefore, SRB1 was found abundantly expressed in pig ECs and its expression was not influenced by incubation with HDL. Finally, blockade of SRB1 in HDL- and PBS-incubated cells led to comparable up-regulation in SRB1 levels (Supplementary material online, Figure S3).

To further confirm the transfer of miR-126-5p and -3p from HC-HDL to the ECs, we analysed pre-miR-126 and EGFL7 levels. As shown in Figure 3, both pre-miR-126 (Figure 3C) and EGFL7 (Figure 3D) were similarly expressed among all the three groups excluding an enhanced

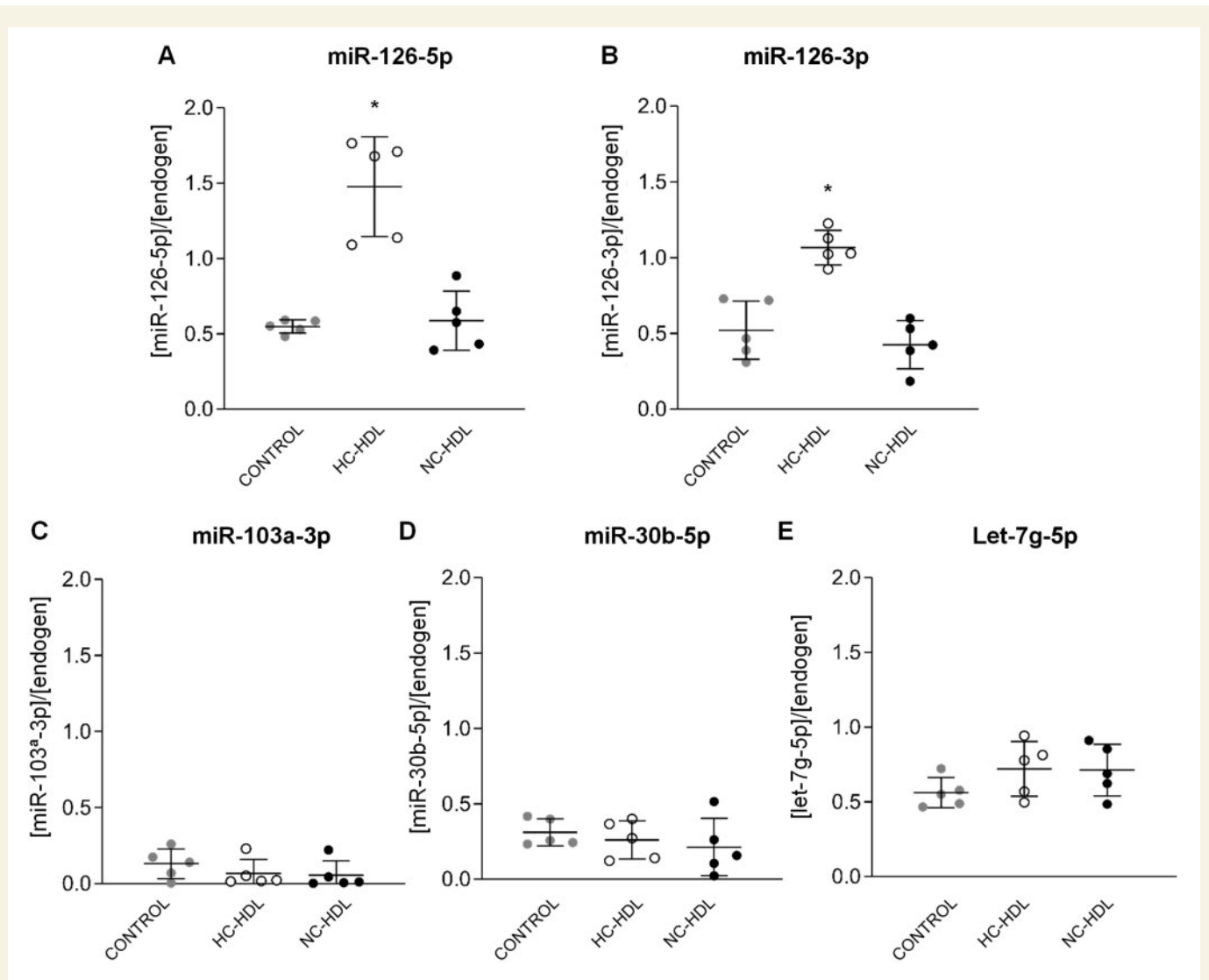


Figure 2 Endothelial cells incubated with hypercholesterolaemic-HDL show higher miR-126-5p and 3p levels as compared to normocholesterolaemic-HDL [miR126-5p (A) and miR126-3p (B)], whereas no differences were observed for 103a-3p (C), miR-30b-5p (D), or let-7g-5p (E) levels. $n = 5$. Data are reported as mean \pm SD. *ANOVA test $P < 0.05$ vs. Control and NC-HDL groups. HC: hypercholesterolaemic; NC: normocholesterolaemic.

intracellular transcription of miRNA-126 in HC-HDL-treated cells and confirming transfer from HC-HDL.

3.4 miR-126 target genes on ECs

We used different computational databases (Supplementary material online, Figure S4 and Table S6) to identify potential target genes of miR-126-5p and -3p in ECs, and only those identified in at least two databases were further investigated. We identified a total of 7597 candidate target genes potentially regulated by miR-126 (3p-strands: 454; 5p-strands: 7143). Among them, common target genes were identified from at least two databases (51 for miR-126-3p and 942 for miR-126-5p). HIF1 α was the potential best target gene for miR-126-5p regulation given the low MFE values (-8.3, -11.2, -12.6, -12.1, -8.5, -13.1 Kcal/mol) and its six tentative binding sites for miR126-5p (Table 1). The best potential target for miR126-3p was DR5 but it could not be validated because its sequence is not yet available in *S. Scrofa*.

To further validate HIF1 α as a target gene for miR126, we examined the effects of miR-126-mimics and miR-126-inhibitors (both -5p and -3p) in ECs (Figure 4). Indeed, control ECs transfected with both miR126-mimics showed lower HIF1 α transcript levels and protein expression than ECs transfected with the negative control and both miR126-inhibitors (Figure 4A–D and Supplementary material online, Figure S5). HIF1 α gene expression was lower in negative-control transfected ECs incubated with HC-HDLs as compared to NC-HDL and control ($P < 0.05$; Figure 4E and F and Supplementary material online, Figure S5). In the EC cultures treated with HDL the effects of HL-HDL on the down-regulation of HIF1 α expression were abrogated by miR126-5p/3p inhibitors (Supplementary material online, Figure S6).

Based on these findings, we proceeded to validate HIF1 α by qPCR ($n = 5$) and found that HIF1 α transcript levels were significantly down-regulated in ECs treated with HC-HDL ($P < 0.01$ vs. PBS/control; $P < 0.006$ vs. NC-HDL; Figure 5A). HIF1 α protein levels were also significantly reduced in HC-HDL treated ECs (Figure 5B).

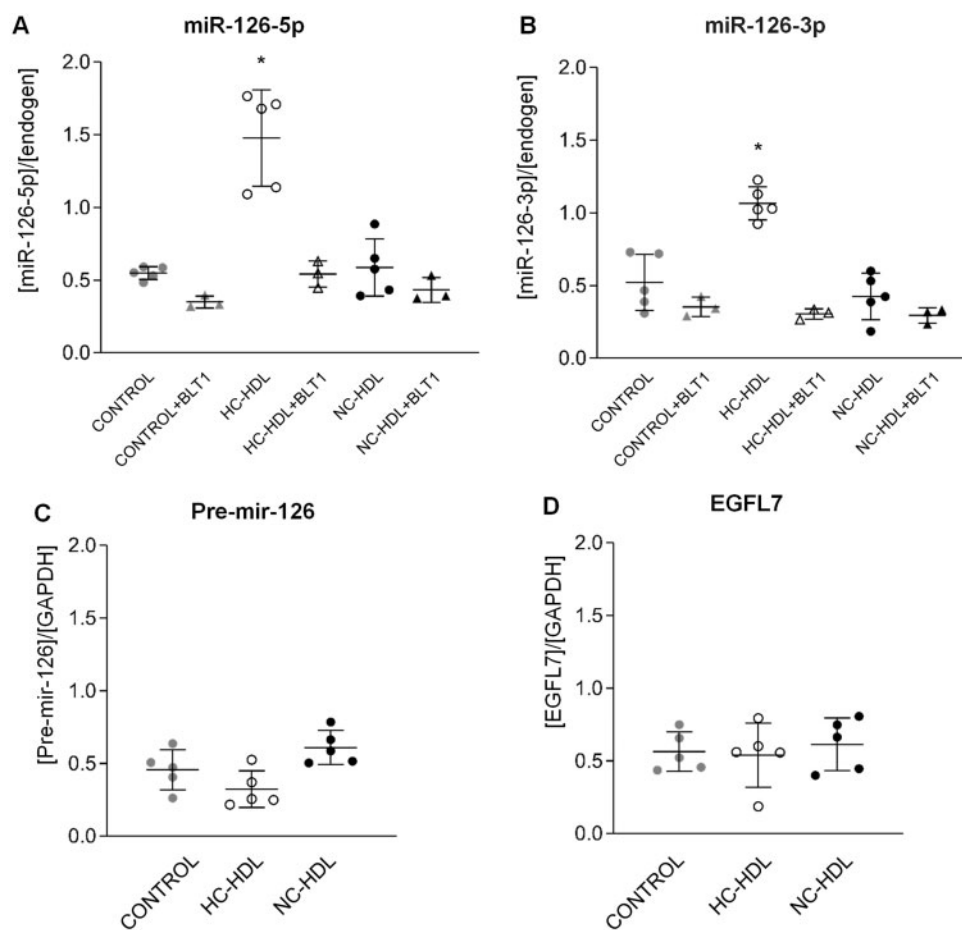


Figure 3 Hypercholesterolaemic HDL particles transfer miR-126-5p and -3p (A and B, respectively) to endothelial cells through a SRB1-dependent mechanism. No differences are detected for Pre-miR-126 (C) or for miR-126 encoding gene EGFL7 (D) levels among the different groups. $n = 5$. Data are reported as mean \pm SD. *ANOVA test $P < 0.05$ vs. any other group. HC: hypercholesterolaemic; NC: normocholesterolaemic.

Mimic-MiR126 (-5p and -3p) induced down-regulation of VCAM1 mRNA expression (Supplementary material online, Figure S7A and B) and up-regulation of VEGFA mRNA expression (Supplementary material online, Figure S7C and D).

3.5 *In vivo* validation of HC-HDL-related miR-126 potential to modulate endothelial HIF1 α

Finally, to determine whether our *in vitro* findings translated into the *in vivo* setting, we assessed HIF1 α expression by confocal microscopy in the coronary arteries of NC pigs administered HC- or NC- HDLs. Interestingly, as shown in Figure 6, expression of HIF1 α was markedly reduced in the intimal layer of the coronary arteries of those NC animals administered HC-HDLs as compared to those administered NC-HDLs.

4. Discussion

In the present study, we report that: (i) HDL formed in hypercholesterolaemic conditions transport different amounts of miRNAs than those HDL formed in normocholesterolaemic conditions; (ii) miR-126-5p and

-3p content is higher in HC-HDL particles; (iii) HC-HDL transfer miR-126 to ECs through a SRB1-dependent mechanism; (iv) internalized miRNA-126 regulates HIF1 α in recipient cells. HIF1 α down-regulation is observed *in vivo* as seen in the coronary arteries of animals treated with HL-HDL but not in animals treated with NL-HDL.

During the last years, it has become increasingly evident that HDL can transport multiple miRNAs including miR-126²⁹, miR-103³⁰, let-7g, miR-222, and miR-223⁶ among others. However, it remained to be determined whether the presence of cardiovascular risk factors altered the HDL transported miRNA signature. In the present study, we demonstrate that HDL formed under hypercholesterolaemic conditions, because of high dietary fat intake, show a higher abundance of the miRNAs miR-126-5p and -3p, and miR-30b-5p and, conversely, a lower amount of miRNAs miR-103a-3p and let-7g-5p as compared to those HDL formed in a normocholesterolaemic milieu. Interestingly, Vickers et al.⁶ had reported a differential HDL-miRNA signature (particularly miR223 levels) in familial hypercholesterolaemia patients that have high LDL-cholesterol levels during life, due to the inherited condition of the disease. So far, a positive association between miR-126 levels in plasma and in HDL has been described, as well as in coronary artery disease and myocardial infarction.^{29,31,32} Furthermore, higher amount of miR-126

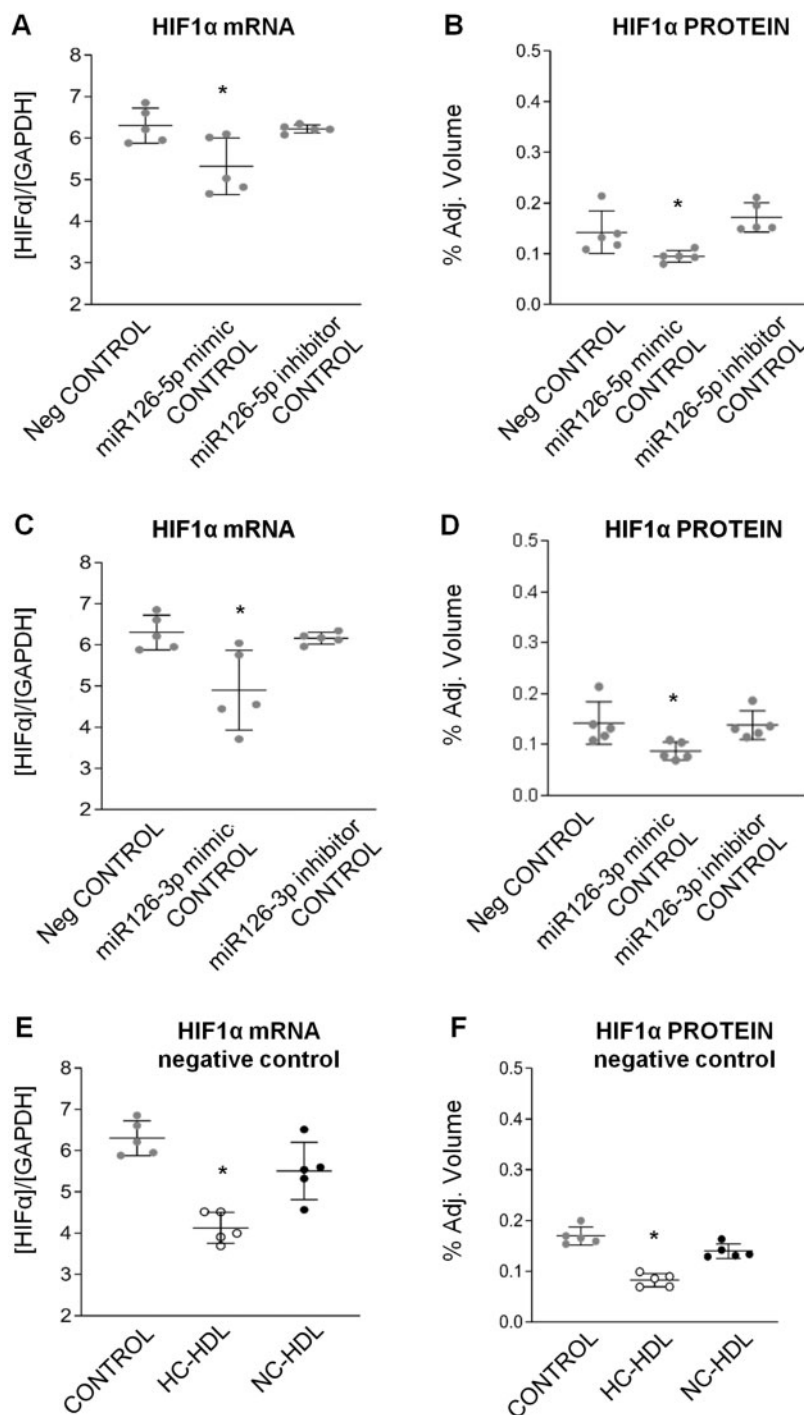


Figure 4 Control ECs transfected with miR126-mimic show lower HIF1 α gene levels as compared to ECs transfected with the negative control both at mRNA expression and protein level (A–D). HIF1 α -mRNA expression was lower in negative-control transfected ECs incubated with HC- as compared to NC-HDLs and control (E and F). *ANOVA test $P < 0.05$. HC: hypercholesterolaemic; NC: normocholesterolaemic.

was found in HDL particles of overweight and obese subjects,^{33,34} and we have recently shown that miR-126 regulates monocyte/macrophage differentiation under a rich LDL-cholesterol environment.²⁸ Indeed, a positive association between miR-126 expression and LDL-cholesterol levels has been demonstrated.³⁵ Here, we demonstrate that HDL particles formed in a diet-induced hypercholesterolaemic milieu with high

LDL-cholesterol levels carry a high content of miR-126, which is delivered into ECs via a SRB1, leading to the down-regulation of its target gene HIF-1 α . As such, SRB1 blockade inhibited miR-126 (both -5p and -3p) delivery into ECs pointing to the critical role of this receptor in HDL-miRNA internalization into target recipient cells. This finding is further supported by the fact that no changes are detected in pre-miR-126

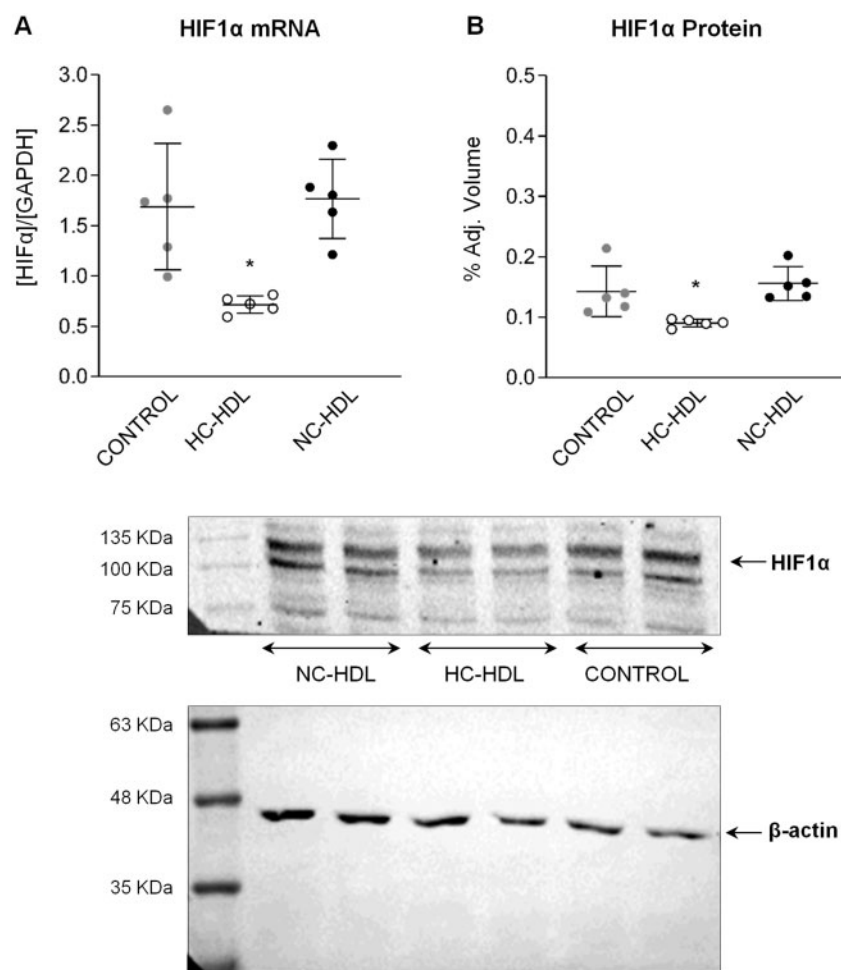


Figure 5 mRNA expression and protein levels of miR126 target HIF1 α in endothelial cells. $n=5$. Data are reported as mean \pm SD. *ANOVA test $P < 0.05$ vs. Control and NC-HDL groups. HC: hypercholesterolaemic; NC: normocholesterolaemic.

(mir-126) or its encoding gene EGFL7.³⁶ SRB1 is a membrane receptor involved in the selective uptake of cholesteryl ester from HDL. SRB1 is highly expressed in the liver and other cells including monocytes/macrophages, ECs, smooth muscle cells, adipocytes, and steroidogenic cells.^{37–39} The ability of HDL particles to transfer cargo-miRNAs into recipient cells via SRB1 had already been described in macrophages and hepatocytes.⁶ In fact, Vickers et al.⁶ reported that SRB1 over expression associated with the greatest cellular uptake of HDL-miRNAs.

Whereas in rodents SRB1 is expressed most abundantly in tissues that efficiently utilize cholesterol ester (biliary cholesterol secretion or steroid hormone production),⁴⁰ in humans SRB1 is homogeneously distributed in all cells.⁴¹ In the present study, we show that in pigs there are comparable SRB1 expression levels in the liver and arterial beds. It is possible that SRB1 serves as docking receptor for HDL to transfer their miRNA-cargo into target cells. Although the SRB1 is the endothelial receptor mainly involved in HDL-miRNA transfer, we cannot exclude that other HDL receptors (ABCA1, ABCG1) may also be involved in HDL-miR126 transfer to ECs.⁴²

The role of miR-126 on the cardiovascular system is controversial, with opposed results in different studies. miR-126 has shown to regulate

angiogenesis and blood vessel integrity by directly repressing the Sprouty Related EVH1 Domain Containing 1 (SPRED1)⁴³ gene and the phosphoinositide-3-kinase regulatory subunit 2^{44,45} with the consequent increase in VEGFA.⁴⁶ Moreover, miR-126 has also shown to reduce leucocyte adherence and vascular inflammation by targeting VCAM-1.⁴⁷ On the other hand, LDL-cholesterol and miRNA-126 levels are positively associated in patients with asymptomatic coronary artery disease and have been suggested to exert prognostic value for future cardiovascular events.⁴⁸ In line with previous work, we further confirm the ability of miR-126 to down-regulate endothelial VCAM-1 expression and indirectly enhance VEGFA transcript levels; yet, we further demonstrate the ability of both miR-126s' (5p and 3p) to reduce endothelial HIF1 α gene levels. Moreover, our *in vitro* findings are further recapitulated *in vivo* where HIF1 α protein levels are lower in the intima of the coronary arteries of hypercholesterolaemic pigs. Although the complexity of the *in vivo* model does not allow to exclude the existence of other potential mechanisms modulating HIF-1 α , all animals were kept under identical conditions except for the type of infused HDL. It is, therefore, plausible to consider that the changes observed in endothelial HIF1 α may derive from HC-HDL-miR126 transfer. HIF1 α is a transcription factor that

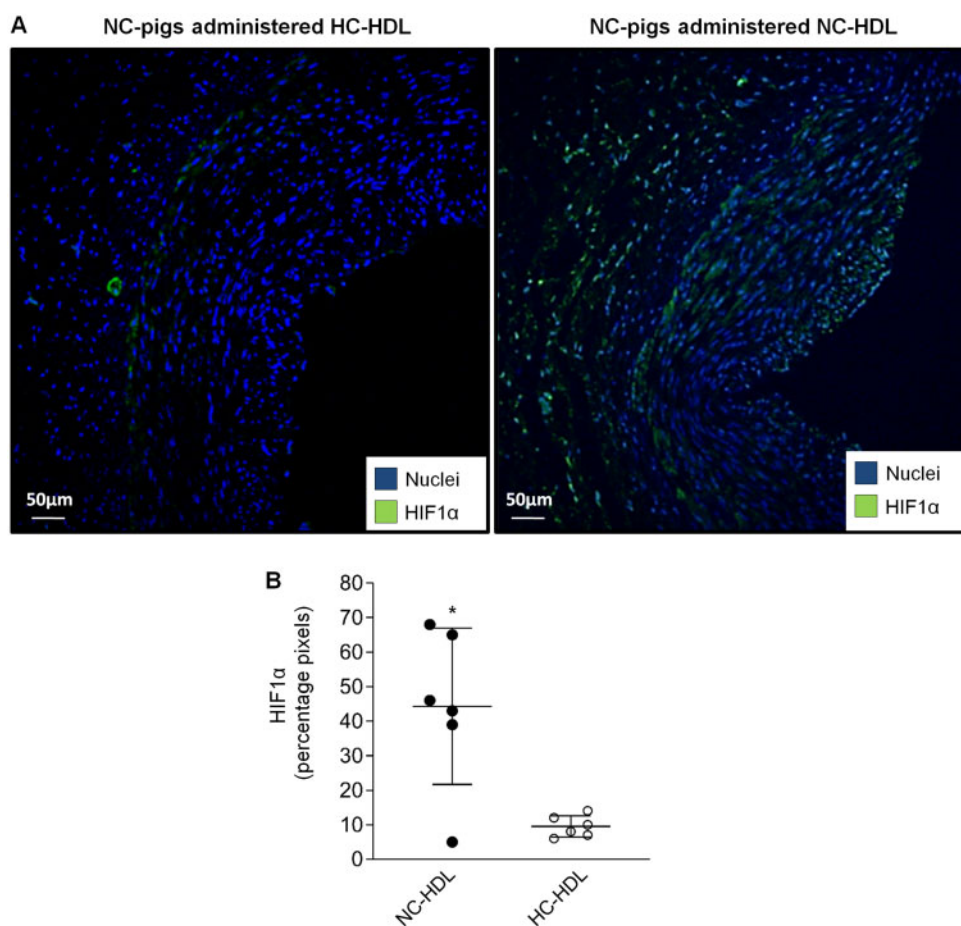


Figure 6 Confocal microscopy analysis of HIF-1 α detection in the endothelial layer of the coronary artery of normocholesterolaemic (NC) pigs administered NC- or hypercholesterolaemic (HC)-HDLs. Representative images of HIF1 α (green) detection (A) and bar-graph quantification (B). Data are reported as mean \pm SD. $n = 6$ animals/group. *T-test $P < 0.05$ vs. NC pigs administered HC-HDL.

serves as a hypoxia sensor to induce the expression of angiogenic genes. Yet, under normoxic conditions, HIF1 α is known to modulate compensatory and adaptive mechanisms. In this regard, Liu *et al.*⁴⁹ have recently described in cancer cells that suppression of miR-126 increases HIF1 α expression promoting metastasis and therapeutic resistance. We evidence, in ECs, that overexpression of miR-126 reduces HIF1 α expression likely interfering with metabolic adaptation, innate immune response, survival and apoptosis.⁵⁰ On the other hand, HIF1 α has been described to be modulated, under hypoxic conditions, by miR-155,⁵¹ miR-18a, miR-199a, miR-429, miR-433,⁵² and miR-497~195.^{53,54} The exact mechanism by which HDL are loaded with miR-126 under hypercholesterolaemic condition is not known. Biophysical studies have suggested that dipolar lipids facilitate small RNAs incorporation within HDL particles.⁵⁵ In this regard, we could speculate that the reported changes in lipid composition observed in HC-HDL particles²⁰ may have favoured miR-126 association to circulating HDLs. Yet, further studies are needed to confirm this hypothesis and determine the relevance of modulating miR-126 expression in the vascular wall. In this regard, the *in vivo* functional impact of miR-126/HIF1 α deserves to be investigated.

In conclusion, we demonstrate that diet-induced hypercholesterolaemia leads to alterations in HDL-miRNA profile favouring an enrichment

in miR-126 that can be delivered to ECs interfering with key vascular functions. Collectively, our data provides further insights as to the impact of hypercholesterolaemia on HDL biogenesis, HDL biology, and HDL composition as well as on the potential outcomes on HDL-miRNA intercellular communication. Whether miR-126 may serve as a potential therapeutic target or whereas reversing hypercholesterolaemia (statin treatment, diet approaches) may restore HDL-related miRNA normal profile deserve to be investigated.

Supplementary material

Supplementary material is available at *Cardiovascular Research* online.

Conflict of interest: none declared.

Acknowledgements

We gratefully acknowledge the valuable help and support of M.A. Canovas, P. Catalina, O.García, J. Moreno, L. Nasarre, F.J. Rodriguez, and M. Pescador with animal handling and for the proper conduct of all the experimental and molecular work.

Table 1 miR-126 target genes by *in silico* analysis

miR-126-5p target genes		Cellular functions by core analysis, a tool from IPA (Ingenuity Pathway Analysis). The cellular functions are showed by P-values according to score. Minimum Free Energy (MFE) values were obtained by RNAhybrid. Bold HIF1α MFE highlighted in bold.									
Top-10 miR-126-5p target genes	Cell cycle	Cell morphology	Lipid metabolism	Cellular movement	Cellular assembly and organization	Cellular development	Cellular growth and proliferation	Cell-to-cell signalling and interaction	Total score	MFE values	
HGF	2	9	1	9	3	8	1	7	40	-9.4	
IL6	6	4	0	2	3	10	2	2	29	-12.5	
CD44	2	4	0	7	0	5	1	4	23	-12.6	
ADIPOQ	1	1	0	2	4	5	3	1	17	-8.9	
BDNF	0	4	0	4	3	4	0	1	16	-9.7	
BCL2	3	4	0	0	0	3	3	1	14	-13.1	
NRG1	3	0	0	2	3	5	0	1	14	-11	
HIF1A	4	0	0	3	0	5	0	0	12	-11.2	
ITGA4	0	2	0	6	3	0	0	1	12	-12.1	
MAD2L1	9	0	0	0	3	0	0	0	12	-17.9	
P-value	0.000046	0.000048	0.000295	0.000597	0.000756	0.00179	0.00179	0.00197		-10.9	

The potential target genes for miR-126-5p related with the top 10 cellular functions by core analysis, a tool from IPA (Ingenuity Pathway Analysis). The cellular functions are showed by P-values according to score. Minimum Free Energy (MFE) values were obtained by RNAhybrid. Bold HIF1α MFE highlighted in bold.

Funding

This work was supported by the Plan Nacional de Salud (PNS) [PGC2018-094025-B-I00 to G.V and SAF2016-76819-R to L.B.] from the Spanish Ministry of Science and Innovation and funds FEDER 'Una Manera de Hacer Europa'; a grant from the Spanish Society of Cardiology (Beca FEC Investigación Básica/2016 to G.V); the Instituto de Salud Carlos III (ISCIII) [P17/01321 to G.A.]; and CIBERCV (to L.B). We thank the support of the Generalitat of Catalunya (Secretaria d'Universitats i Recerca del Departament d'Economia i Coneixement de la Generalitat, 2017 SGR 1480) and the Fundación Investigación Cardiovascular-Fundación Jesus Serra for their continuous support.

References

- He L, Hannon GJ. Erratum: microRNAs: small RNAs with a big role in gene regulation. *Nat Rev Genet* 2004;**5**:522–531.
- Kontush A, Lindahl M, Lhomme M, Calabresi L, Chapman MJ, Davidson WS. Structure of HDL: particle subclasses and molecular components. In Barrett, JE. (ed.) *Handbook of Experimental Pharmacology*. Switzerland: Springer Nature; 2015. p. 3–51.
- Badimon L, Vilahur G. LDL-cholesterol versus HDL-cholesterol in the atherosclerotic plaque: inflammatory resolution versus thrombotic chaos. *Ann N Y Acad Sci* 2012;**1254**:18–32.
- Theilmeyer G, Schmidt C, Herrmann J, Keul P, Schäfers M, Herrgott I, Mersmann J, Larmann J, Hermann S, Stypmann J, Schober O, Hildebrand R, Schulz R, Heusch G, Haude M, von Wnuck Lipinski K, Herzog C, Schmitz M, Erbel R, Chun J, Levkau B. High-density lipoproteins and their constituent, sphingosine-1-phosphate, directly protect the heart against ischemia/reperfusion injury *in vivo* via the S1P3 lysophospholipid receptor. *Circulation* 2006;**114**:1403–1409.
- Kontush A. HDL-mediated mechanisms of protection in cardiovascular disease. *Cardiovasc Res* 2014;**103**:341–349.
- Vickers KC, Palmisano BT, Shoucri BM, Shamburek RD, Remaley AT. MicroRNAs are transported in plasma and delivered to recipient cells by high-density lipoproteins. *Nat Cell Biol* 2011;**13**:423–433.
- Michell DL, Vickers KC. Lipoprotein carriers of microRNAs. *Biochim Biophys Acta* 2016;**1861**:2069–2074.
- Condorelli G, Latronico MVG, Cavarretta E. microRNAs in cardiovascular diseases: current knowledge and the road ahead. *J Am Coll Cardiol* 2014;**63**:2177–2187.
- Urbich C, Kuehnbacher A, Dimmeler S. Role of microRNAs in vascular diseases, inflammation, and angiogenesis. *Cardiovasc Res* 2008;**79**:581–588.
- Doggrell SA. No cardiovascular benefit with evacetrapib—is this the end of the road for the 'cetrapibs'? *Expert Opin Pharmacother* 2017;**18**:1439–1442.
- Fisher EA, Feig JE, Hewing B, Hazen SL, Smith JD. High-density lipoprotein function, dysfunction, and reverse cholesterol transport. *Arterioscler Thromb Vasc Biol* 2012;**32**:2813–2820.
- Nicholls SJ, Lundman P, Harmer JA, Cutri B, Griffiths KA, Rye K-A, Barter PJ, Celermajer DS. Consumption of saturated fat impairs the anti-inflammatory properties of high-density lipoproteins and endothelial function. *J Am Coll Cardiol* 2006;**48**:715–720.
- Kontush A, Chapman MJ. Functionally defective high-density lipoprotein: a new therapeutic target at the crossroads of dyslipidemia, inflammation, and atherosclerosis. *Pharmacol Rev* 2006;**58**:342–374.
- Navab M, Reddy ST, Lenten BJ, Van, Fogelman AM. HDL and cardiovascular disease: atherogenic and atheroprotective mechanisms. *Nat Rev Cardiol* 2011;**8**:222–232.
- Holy EW, Besler C, Reiner MF, Camici GG, Manz J, Beer JH, Lüscher TF, Landmesser U, Tanner FC. High-density lipoprotein from patients with coronary heart disease loses anti-thrombotic effects on endothelial cells: impact on arterial thrombus formation. *Thromb Haemost* 2014;**112**:1024–1035.
- Sorrentino SA, Besler C, Rohrer L, Meyer M, Heinrich K, Bahlmann FH, Mueller M, Horváth T, Doerries C, Heinemann M, Flemmer S, Markowski A, Manes C, Bahr MJ, Haller H, von Eckardstein A, Drexler H, Landmesser U. Endothelial-vasoprotective effects of high-density lipoprotein are impaired in patients with type 2 diabetes mellitus but are improved after extended-release niacin therapy. *Circulation* 2010;**121**:110–122.
- Riwanto M, Rohrer L, Roschitzki B, Besler C, Mocharla P, Mueller M, Perisa D, Heinrich K, Altwegg L, Eckardstein A, von, Luscher TF, Landmesser U. Altered activation of endothelial anti- and proapoptotic pathways by high-density lipoprotein from patients with coronary artery disease: role of high-density lipoprotein-proteome remodeling. *Circulation* 2013;**127**:891–904.
- Zewinger S, Kleber ME, Rohrer L, Lehmann M, Triem S, Jennings RT, Petrakis I, Dressel A, Lepper PM, Scharnagl H, Ritsch A, Thorand B, Heier M, Meisinger C, de las Heras Gala T, Koenig W, Wagenpfeil S, Schwedhelm E, Böger RH, Laufs U, von Eckardstein A, Landmesser U, Lüscher TF, Fliser D, März W, Meinitzer A, Speer T. Symmetric dimethylarginine, high-density lipoproteins and cardiovascular disease. *Eur Heart J* 2017;**38**:1597–1607.

19. Vilahur G, Gutiérrez M, Casani L, Cubedo J, Capdevila A, Pons-Llado G, Carreras F, Hidalgo A, Badimon L. Hypercholesterolemia abolishes high-density lipoprotein-related cardioprotective effects in the setting of myocardial infarction. *J Am Coll Cardiol* 2015;**66**:2469–2470.
20. Padró T, Cubedo J, Camino S, Béjar MT, Ben-Aicha S, Mendieta G, Escolà-Gil JC, Escate R, Gutiérrez M, Casani L, Badimon L, Vilahur G. Detrimental effect of hypercholesterolemia on high-density lipoprotein particle remodeling in pigs. *J Am Coll Cardiol* 2017;**70**:165–178.
21. Kilkenny C, Browne WJ, Cuthill IC, Emerson M, Altman DG. Improving bioscience research reporting: the ARRIVE guidelines for reporting animal research. *PLoS Biol* 2010;**8**:e1000412.
22. Vilahur G, Casani L, Peña E, Juan-Babot O, Mendieta G, Crespo J, Badimon L. HMG-CoA reductase inhibition prior reperfusion improves reparative fibrosis post-myocardial infarction in a preclinical experimental model. *Int J Cardiol* 2014;**175**:528–538.
23. Cremer SE, Krogh AKH, Hedström MEK, Christiansen LB, Tarnow I, Kristensen AT. Analytical validation of a flow cytometric protocol for quantification of platelet microparticles in dogs. *Vet Clin Pathol* 2018;**47**:186–196.
24. Rodríguez C, Martínez-González J, Sánchez-Gómez S, Badimon L. LDL downregulates CYP51 in porcine vascular endothelial cells and in the arterial wall through a sterol regulatory element binding protein-2-dependent mechanism. *Circ Res* 2001;**88**:268–274.
25. Yu M, Romer KA, Nieland TJF, Xu S, Saenz-Vash V, Penman M, Yesilaltay A, Carr SA, Krieger M. Exoplasmic cysteine Cys384 of the HDL receptor SR-BI is critical for its sensitivity to a small-molecule inhibitor and normal lipid transport activity. *Proc Natl Acad Sci USA* 2011;**108**:12243–12248.
26. Das MK, Andreassen R, Haugen TB, Furu K. Identification of endogenous controls for use in miRNA quantification in human cancer cell lines. *Cancer Genomics Proteomics* 2016;**13**:63–68.
27. Kruger J, Rehmsmeier M. RNAhybrid: microRNA target prediction easy, fast and flexible. *Nucleic Acids Res* 2006;**34**:W451–W454.
28. Escate R, Padro T, Badimon L. LDL accelerates monocyte to macrophage differentiation: effects on adhesion and anoikis. *Atherosclerosis* 2016;**246**:177–186.
29. Choteau SA, Cuesta Torres LF, Barraclough JY, Elder AMM, Martínez GJ, Chen Fan WY, Shrestha S, Ong KL, Barter PJ, Celermajer DS, Rye K-A, Patel S, Tabet F. Transcoronary gradients of HDL-associated MicroRNAs in unstable coronary artery disease. *Int J Cardiol* 2018;**253**:138–144.
30. Michell DL, Vickers KC. HDL and microRNA therapeutics in cardiovascular disease. *Pharmacol Ther* 2016;**168**:43–52.
31. Wagner J, Riwanto M, Besler C, Knau A, Fichtlscherer S, Roxe T, Zeiher AM, Landmesser U, Dimmeler S. Characterization of levels and cellular transfer of circulating lipoprotein-bound MicroRNAs. *Arterioscler Thromb Vasc Biol* 2013;**33**:1392–1400.
32. Zampetaki A, Willeit P, Tilling L, Drozdov I, Prokopi M, Renard J-M, Mayr A, Weger S, Schett G, Shah A, Boulanger CM, Willeit J, Chowienzyk PJ, Kiechl S, Mayr M. Prospective study on circulating MicroRNAs and risk of myocardial infarction. *J Am Coll Cardiol* 2012;**60**:290–299.
33. Tabet F, Cuesta Torres LF, Ong KL, Shrestha S, Choteau SA, Barter PJ, Clifton P, Rye K-A. High-density lipoprotein-associated miR-223 is altered after diet-induced weight loss in overweight and obese males. *PLoS One* 2016;**11**:e0151061.
34. Krause BJ, Carrasco-Wong I, Dominguez A, Arnaiz P, Fariás M, Barja S, Mardones F, Casanello P. Micro-RNAs Let7e and 126 in plasma as markers of metabolic dysfunction in 10 to 12 years old children. *PLoS One* 2015;**10**:e0128140.
35. Sezer Zhmurov Ç, Timirci-Kahraman Ö, Amadou FZ, Fazloğulları O, Başaran C, Catal T, Zeybek Ü, Bermek H. Expression of *Egfl7* and miRNA-126-5p in symptomatic carotid artery disease. *Genet Test Mol Biomarkers* 2016;**20**:125–129.
36. Bartel DP. MicroRNAs: genomics, biogenesis, mechanism, and function. *Cell* 2004;**116**:281–297.
37. Kratzer A, Giral H, Landmesser U. High-density lipoproteins as modulators of endothelial cell functions: alterations in patients with coronary artery disease. *Cardiovasc Res* 2014;**103**:350–361.
38. Nieland TJF, Chroni A, Fitzgerald ML, Maliga Z, Zannis VI, Kirchhausen T, Krieger M. Cross-inhibition of SR-BI- and ABCA1-mediated cholesterol transport by the small molecules BLT-4 and glyburide. *J Lipid Res* 2004;**45**:1256–1265.
39. Krieger M. Charting the fate of the “good cholesterol”: identification and characterization of the high-density lipoprotein receptor SR-BI. *Annu Rev Biochem* 1999;**68**:523–558.
40. Acton S, Rigotti A, Landschulz KT, Xu S, Hobbs HH, Krieger M. Identification of scavenger receptor SR-BI as a high density lipoprotein receptor. *Science* 1996;**271**:518.
41. Calvo D, Gómez-Coronado D, Lasunción MA, Vega MA. CLA-1 is an 85-kD plasma membrane glycoprotein that acts as a high-affinity receptor for both native (HDL, LDL, and VLDL) and modified (OxLDL and AcLDL) lipoproteins. *Arterioscler Thromb Vasc Biol* 1997;**17**:2341.
42. Röhlrl C, Stangl H. HDL endocytosis and resecretion. *Biochim Biophys Acta* 2013;**1831**:1626–1633.
43. Mathiyalagan P, Liang Y, Kim D, Misener S, Thorne T, Kamide CE, Klyachko E, Losordo DW, Hajjar RJ, Sahoo S. Angiogenic mechanisms of human CD34⁺ stem cell exosomes in the repair of ischemic hindlimb. *Circ Res* 2017;**120**:1466–1476.
44. Chen L, Wang J, Wang B, Yang J, Gong Z, Zhao X, Zhang C, Du K. MiR-126 inhibits vascular endothelial cell apoptosis through targeting PI3K/Akt signaling. *Ann Hematol* 2016;**95**:365–374.
45. Fish JE, Santoro MM, Morton SU, Yu S, Yeh R-F, Wythe JD, Ivey KN, Bruneau BG, Stainier D, Srivastava D. miR-126 regulates angiogenic signaling and vascular integrity. *Dev Cell* 2008;**15**:272–284.
46. Donnem T, Lonvik K, Eklo K, Berg T, Sorbye SW, Al-Shibli K, Al-Saad S, Andersen S, Stenvold H, Bremnes RM, Busund L-T. Independent and tissue-specific prognostic impact of miR-126 in non-small cell lung cancer. *Cancer* 2011;**117**:3193–3200.
47. Harris TA, Yamakuchi M, Ferlito M, Mendell JT, Lowenstein CJ. MicroRNA-126 regulates endothelial expression of vascular cell adhesion molecule 1. *Proc Natl Acad Sci USA* 2008;**105**:1516–1521.
48. Sun X, Zhang M, Sanagawa A, Mori C, Ito S, Iwaki S, Satoh H, Fujii S. Circulating microRNA-126 in patients with coronary artery disease: correlation with LDL cholesterol. *Thrombosis J* 2012;**10**:16.
49. Liu W, Chen H, Wong N, Haynes W, Baker CM, Wang X. Pseudohypoxia induced by miR-126 deactivation promotes migration and therapeutic resistance in renal cell carcinoma. *Cancer Lett* 2017;**394**:65–75.
50. Kuschel A, Simon P, Tug S. Functional regulation of HIF-1 α under normoxia-is there more than post-translational regulation? *J Cell Physiol* 2012;**227**:514–524.
51. Nallamshetty S, Chan SY, Loscalzo J. Hypoxia: a master regulator of microRNA biogenesis and activity. *Free Radic Biol Med* 2013;**64**:20–30.
52. Serocki M, Bartoszevska S, Janaszak-Jasiecka A, Ochocka RJ, Collawn JF, Bartoszewski R. miRNAs regulate the HIF switch during hypoxia: a novel therapeutic target. *Angiogenesis* 2018;**21**:183–202.
53. Yang M, Li C-J, Sun X, Guo Q, Xiao Y, Su T, Tu M-L, Peng H, Lu Q, Li Q, He H-B, Jiang T-J, Lei M-X, Wan M, Cao X, Luo X-H. MiR-497~195 cluster regulates angiogenesis during coupling with osteogenesis by maintaining endothelial Notch and HIF-1 α activity. *Nat Commun* 2017;**8**:16003.
54. Bai R, Zhao A-Q, Zhao Z-Q, Liu W-L, Jian D-M. MicroRNA-195 induced apoptosis in hypoxic chondrocytes by targeting hypoxia-inducible factor 1 α . *Eur Rev Med Pharmacol Sci* 2015;**19**:545–551.
55. Lu D, Rhodes DG. Binding of phosphorothioate oligonucleotides to zwitterionic liposomes. *Biochim Biophys Acta* 2002;**1563**:45–52.

Translational perspectives

Clinical trials aimed at increasing high-density lipoprotein (HDL)-cholesterol in secondary prevention have resulted disappointing. Furthermore, studies have reported on the negative impact of cardiovascular disease on HDL composition and function. The structural/functional changes that suffer HDL particles under cardiovascular comorbid pathological conditions need to be investigated because they render them dysfunctional and even deleterious. We evidence that diet-induced hypercholesterolaemia (the most prevalent cardiovascular risk factor) alters HDL miRNA signature and these altered miRNAs directly affect vascular homeostasis, adversely regulating the vascular response. Identifying the remodelling changes affecting HDL particles due to pathological conditions will open new avenues for therapeutic intervention.